Available online at www.sciencedirect.com
SCIENCE DIRECT
Journal of Chromatography A, 1109 (2006) 167–173
JOURNAL OF CHROMATOGRAPHY A
www.elsevier.com/locate/chroma

Structural transition of glucagon in the concentrated solution observed by electrophoretic and spectroscopic techniques

Satomi Onoue [a,d,*], Sumiko Iwasa [a], Takashi Kojima [b], Fumie Katoh [b], Kazuhiro Debari [c], Keitatsu Koh [c], Yoshihisa Matsuda [b], Takehiko Yajima [a]

[a] *Department of Analytical Chemistry, Faculty of Pharmaceutical Sciences, Toho University, Funabashi, Chiba 274-8510, Japan*
[b] *Department of Pharmaceutical Technology, Kobe Pharmaceutical University, Higashi-Nada, Kobe 658-8558, Japan*
[c] *Laboratory of Electron Microscopy, Showa University School of Medicine, Shinagawa, Tokyo 142-8555, Japan*
[d] *Analytical Research and Development, Pfizer Global Research and Development, Nagoya Laboratories, Pfizer Japan Inc., 5-2 Taketoyo, Aichi 470-2393, Japan*

Available online 20 December 2005

Abstract

Glucagon, a polypeptide hormone consisting of 29 amino acid residues, tends to form gel-like fibrillar aggregates, and the glucagon fibril, as well as other pathologically related fibrils including prion, amylin, and β-amyloid, have been found to be cytotoxic through the activation of apoptotic signaling pathways. To understand the aggregation properties of glucagon fibril, we have characterized and compared the physicochemical properties of glucagon, secretin, a member of the glucagon superfamily, and amylin using analytical techniques including capillary electrophoresis (CE), circular dichroism (CD), FT-IR, FT-Raman, transmission electron microscopy (TEM), and β-sheet-imaging probe. Aging treatment of glucagon resulted in the formation of fibrillar aggregates in time- and concentration-dependent manner, and FT-IR and FT-Raman analyses showed the spectral shift of amide I band, suggesting the conformational changes from α-helix to β-sheet structure. Interestingly, secretin, having high sequential and secondary structural homology with glucagon, did not generate the fibrillar aggregates at the conditions tested. In addition, we evaluated the association state of glucagon at various pHs raging from pH 2.0 to 3.5 using CE. Based on the CE data, the rate constants of glucagon aggregation were calculated to be 0.002 ± 0.004/h and 0.080 ± 0.011/h for aging at pH 2.0 and 3.5, respectively, suggesting the pH dependence of self-association. CE showed the potential to separate and detect the glucagon aggregates and intermediates during aging process.

Keywords: Glucagon; Secretin; Fibril; Capillary electrophoresis; FT-IR; FT-Raman

1. Introduction

Conformational diseases, including Alzheimer's disease, type II (non-insulin-dependent) diabetes mellitus, Creutzfeldt-Jakob disease, spongiform encephalopathy, and Huntington's disease, are recognized as complex disorders, characterized by the polymerization and aggregation of normally innocuous and soluble proteins/peptides such as β-amyloid, amylin, prion and polyglutamine [1–6]. The aggregation of these pathologically related amyloidogenic proteins/peptides generate insoluble and toxic fibrils, and they share a distinct conformational feature in the richness of the β-sheet structure [7,8]. There are similarities in physicochemical characteristics such as polarity, hydrophobicity, and the size of side-chain among certain segments containing 10–15 amino acid residues of amyloid-forming peptides/proteins [9,10]. In addition to these pathogenic peptides/proteins, some therapeutic peptides, including insulin [11], GLP-1 analogue [12], and growth hormone [13], also display conformational changes into β-sheet-rich fibrils. These insoluble products are attributed to the formation of partially unfolded intermediates with an exposed hydrophobic region that drives the aggregation towards the physiologically undesirable form [14].

Previously, we have demonstrated that glucagon had an ability to form gel-like fibrillar aggregates, and that glucagon fibrils possessed conformational properties and apoptotic signaling pathways by activating caspases as fibrils derived from pathologically related peptides including β-amyloid and prion [15]. Glucagon, consisting of 29 amino acid residues, plays a central role in the maintenance of normal circulating glucose levels [16],

* Corresponding author. Tel.: +81 569 74 4855; fax: +81 569 74 4748.
E-mail address: Satomi.Onoue@pfizer.com (S. Onoue).

0021-9673/$ – see front matter © 2005 Elsevier B.V. All rights reserved.
doi:10.1016/j.chroma.2005.11.130

and it is widely used for peroral endoscopy, clinical diacrisis and treatment of hypoglycemia. The glucagon injection is usually prepared just prior to administration by dissolving lyophilized glucagon in distilled water to the concentration of 1 mg/ml, therefore, it is a matter of concern that fibrillar formation may occur in the glucagon injection when prepared by inappropriate procedures such as dissolving glucagon in an insufficient volume of water and storing for extended period before administration [15]. Therefore, we strongly emphasize that the instructions supplied by manufacturers should be followed strictly. Secretin is a 27-residue gastrointestinal polypeptide hormone which plays a major role in the regulation of pancreatic exocrine secretin [17], and it is clinically used for diagnosis of pancreatic exocrine dysfunction and gastrinoma. Secretin has primary and secondary structural homology with glucagon [18], so it is a member of the glucagon superfamily which includes the vasoactive intestinal peptide, gastric inhibitory peptide, and pituitary adenylate cyclase activating polypeptide [19]. Although the biological function of secretin has been investigated well, the aggregation property of secretin is not fully elucidated.

It would be of clinical significance to develop analytical methods for monitoring glucagon aggregation and to characterize the properties of aggregated glucagon in order to avoid undesirable side effects in the clinical use. In this investigation, we have characterized and compared the physicochemical properties of glucagon, secretin, and amylin using electrophoretic and spectroscopic techniques including β-sheet-imaging probes, circular dichroism (CD), transmission electron microscopy (TEM), FT-IR, FT-Raman and capillary electrophoresis (CE). Here, we exploit the potential capacity of separation of CE to describe the transition of monomer and oligomer population of glucagon along the fibrillogenic pathway, and thus providing further insights into the associative behavior of glucagon, showing that its non-covalent aggregation was dependent on the condition for storage, especially pH of dissolving buffer.

2. Experimental

2.1. Peptide synthesis

Human glucagon, amylin and porcine secretin (Fig. 1) were chemically synthesized by the solid-phase strategy employing optimal side-chain protection as reported previously [20]. The purity (>98%) of each tested peptide was checked by RP-HPLC, and the pure peptides showed the expected molar ratio of the constituent amino acids in amino acid analysis with a L-8500 amino acid analyzer (Hitachi, Tokyo, Japan). Molecular weight was confirmed with a matrix-assisted laser desorption ionization-time of flight mass spectrometer (Kratos, Manchester, UK).

2.2. Aging treatment of peptides

Glucagon, porcine secretin and amylin were dissolved in 0.01 M HCl at the concentration indicated in the text. Peptides were incubated at 37 °C for the periods indicated in the text and then diluted to the required concentration.

2.3. Congo red binding assay

Congo red-reactive fibrils were measured as described previously [15]. Briefly, aged preparations of peptides were adjusted to a concentration of 1 mg/ml, and 40 μl of each dilution was added to 960 μl of 25 μM Congo red in 20 mM potassium phosphate buffer (pH 7.4) containing 150 mM NaCl. After a 30-min incubation, absorbance was read at 540 and 477 nm, and the concentration of bound Congo red (c_b) was calculated from the equation, $c_b = (A540/25{,}295 - A477/46{,}306)$.

2.4. Transmission electron microscopy (TEM)

An aliquot (2 μl) of the peptide gels or solution was placed on a carbon-coated Formvar 200 mesh nickel grid. The sample was allowed to stand for 15–30 s, and then any excess solution was removed by blotting. The samples were negatively stained with 2% (w/v) uranyl acetate and allowed to dry. The samples were then visualized under an H-7000 transmission electron microscope (Hitachi) operating at 75 kV.

2.5. Circular dichroic analysis of amyloidogenic peptides

Aged preparations of peptides were dissolved in 50% methanol (MeOH)/20 mM Tris–HCl buffer, and circular dichroic (CD) spectra (average of ten scans) were collected from samples (2 ml) at 0.5 nm intervals between the wavelengths of 200 and 400 nm using a J-720 spectropolarimeter (JASCO, Tokyo, Japan). Samples were incubated at room temperature and a baseline spectrum was subtracted from the collected data.

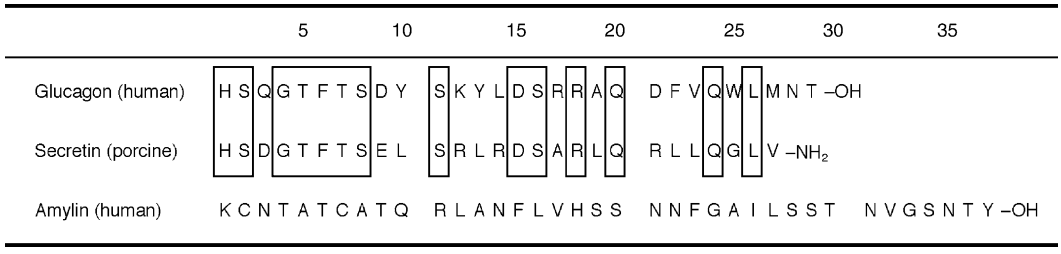

Fig. 1. Amino acid sequence of synthetic peptides. All peptides were chemically synthesized by the solid-phase strategy employing optimal side-chain protection. Identical residues between glucagon and secretin are boxed.

2.6. Spectroscopic analyses of glucagon fibril

Glucagon was dissolved in 0.01 M HCl at the concentration of 5.0 mg/ml, and aged for 24 h at 37 °C. The aged peptide solution was lyophilized, and then the dried sample was subjected to FT-IR and Raman spectroscopic analyses.

For FT-IR spectroscopic analysis, the KBr tablet was prepared by mixing the powder of aged glucagon and KBr crystals. The FT-IR spectra were scanned in the mid-IR region from 4000 to 400 cm^{-1} at intervals of 1 cm^{-1} in an FT/IR-300E spectrometer (JASCO). A pure KBr tablet was used as a blank for background subtraction. The composition of each component in the amide I band of these spectra were estimated quantitatively using the IR Protein Secondary Structure Estimation Program (JASCO) with the minimum standard error [21]. The proportion of a component was computed to be the ratio of the area of the corresponding peak to the sum of the areas of all the peaks.

For FT-Raman spectroscopic analysis, the aged glucagon was set in the hematocrit capillary tube (Drummond Scientific Company, Broomall, PA). FT-Raman spectrum of the aged glucagon was obtained using a FT-Raman 960 spectrometer (Thermo Electron, Waltham, MA), and collected ranging from 30 to 3700 cm^{-1} at a resolution of 4 cm^{-1}. The laser power was less than 1.0 W at the sample position. Data analysis was performed using OMNIC software (Thermo Electron).

2.7. Capillary electrophoresis (CE)

CE analysis was performed on an HP3D capillary electrophoresis system model G1601A (Hewlett-Packard, Wilmington, DE). Conditions were as follows unless noted otherwise: electrophoresis buffer was 0.1 M borate buffer, pH 10, detection was carried out at 214 and 280 nm, and an uncoated fused-silica capillary of 33 cm (effective length 24.5 cm) × 50 μm I.D. was used. Separations were carried out at 8 kV with the anode at the sample injection end of the capillary. Data were collected and processed by the HP ChemStations software (Hewlett-Packard).

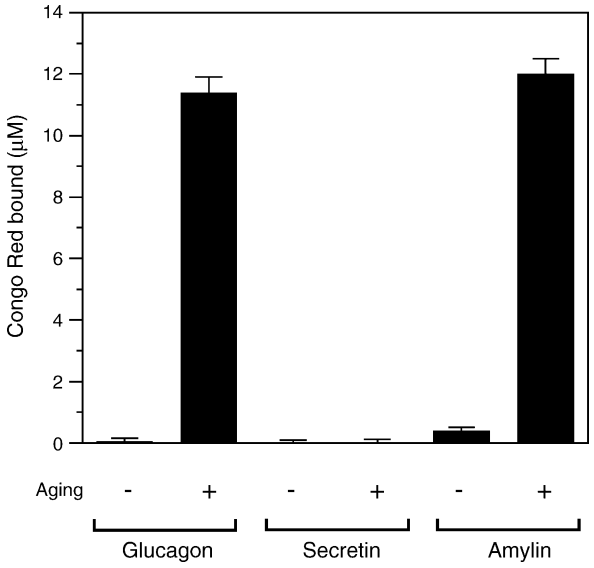

Fig. 2. Aggregation behavior of peptides as monitored by Congo red binding assay. Peptides were incubated at various concentrations (glucagon, 5 mg/ml; secretin, 50 mg/ml; and amylin, 5 mg/ml) in 0.01 M HCl at 37 °C for 24 h, and applied to Congo red-binding assay as described in Section 2.

3. Results and discussions

3.1. Aggregation behavior of peptides

Congo red has been used to detect amyloid fibrils in pathological specimens, since it could bind specifically to amyloid-like aggregates having a β-sheet rich conformation [22]. Aging treatment of glucagon solution at the concentration of 5 mg/ml resulted in the significant generation of amyloid fibril as evidenced by the Congo red staining (Fig. 2). Amylin, an islet amyloid polypeptide, was well known to form cytotoxic aggregates in vitro and in vivo [23], resulting in the induction of type II diabetes mellitus [4], and the amyloidogenic potential of glucagon was found to be similar to that of amylin (Fig. 2). According to TEM image, aged glucagon formed well-defined fibrils (Fig. 3A), whose morphology resembled the aggregates

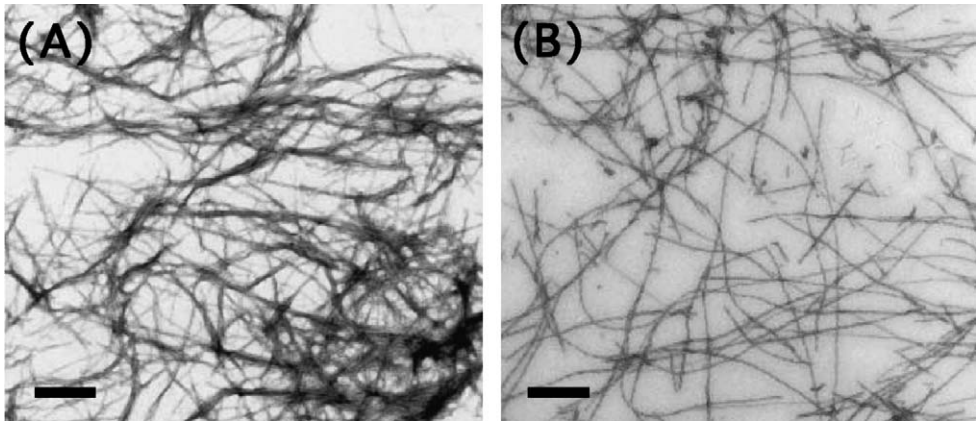

Fig. 3. Electron micrographs of negatively stained fibrils formed by aged glucagon (A) and amylin (B). Fibrils of glucagon and amylin were prepared by aging at the concentration of 5 mg/ml, respectively, in 0.01 M HCl for 24 h. Prior to TEM analysis, the samples were diluted to the final concentration of 1 mg/ml. The bars represent 0.5 μm.

of amylin (Fig. 3B) and other classic amyloid fibrils [24,25]. The fibril morphologies included largely disordered, rigid and branching fibrils stacked together edge to edge with various width and lengths.

In addition to glucagon, aggregation behavior of secretin was also investigated with the use of Congo red binding assay. The primary structure of secretin is highly similar to that of glucagon (Fig. 1). Moreover, their secondary structures, as determined by the NMR and CD spectroscopic investigations [18,26,27], also exhibited similarities. Although secretin and glucagon have structural similarity, aggregation properties of these two peptides were quite different. Secretin, aged at various concentrations ranging from 1 to 50 mg/ml, did not show any signs of fibrillar formation within 24 h aging (Fig. 2), and this was consistent with the TEM image of aged secretin, indicating no fibril or aggregates formation (data not shown). Herein, glucagon displayed the aggregation behavior similar to amylin, having no homology in the primary structure, whereas secretin, a glucagon family peptide, was found to be free from the possibility of aggregation under the conditions tested.

3.2. Spectroscopic analyses of aged glucagon

Structural elucidation of glucagon and secretin has been carried out under variety of conditions in solution [18,26,27]. A general conclusion from these studies is that the two hormones are essentially disordered in aqueous solution, however they adopt a significant amount of amphipathic helical structure in the presence of nonaqueous solvent media.

Generally, the CD spectrum of an α-helical structure shows an intense positive peak at 192 nm and two negative peaks at 209 and 222 nm [28]. The CD spectra of non-aged glucagon and secretin exhibited a typical α-helical structure in hydrophobic condition (50% MeOH/20 mM Tris–HCl buffer, pH 7.4; Fig. 4A and B), and the results were consistent with the previous report [26]. According to the calculation established by Greenfield and Fasman [28], the content of glucagon and secretin were estimated to be 55% and 58%, respectively. Interestingly, aging of glucagon at 5.0 mg/ml resulted in a significant decrease in the α-helical content to ca. 1%. The CD spectrum of a β-sheet structure typically shows an intense positive band at 198 nm and a negative extremal band at 218 nm [23], and the aged glucagon displayed the CD spectral pattern of β-sheet structure. In contrast to glucagon, the CD spectrum of aged secretin at the concentration of 50 mg/ml was almost identical to that of non-aged secretin (Fig. 4B), suggesting no conformational changes during the aging process of these peptides. Non-aged amylin showed a typical α-helical structure in the hydrophobic environment, however, as in the case of glucagon, a conformational transition from an α-helical structure to a β-sheet structure was observed after aging at the concentrations of 5.0 mg/ml (Fig. 4C).

The structural transition of glucagon from an α-helix to a β-sheet structure was also demonstrated by the FT-IR and Raman spectroscopic analyses (Fig. 5A and B). Generally, proteins and peptides secondary structures display signature IR and Raman bands as a consequence of the polypeptides backbone amide

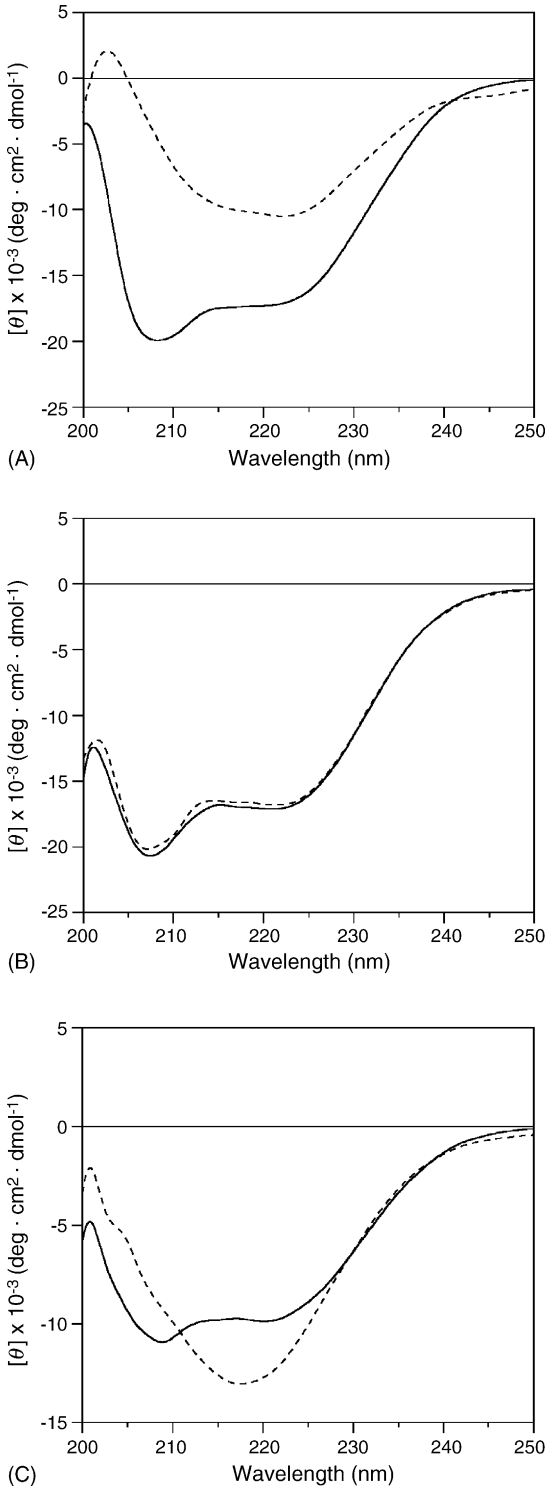

Fig. 4. Typical CD spectra of glucagon, secretin, and amylin. CD spectra of non-aged or aged peptides (A, glucagon at 5.0 mg/ml; B, secretin at 50 mg/ml; and C, amylin at 5.0 mg/ml) were measured in 50% MeOH/20 mM Tris–HCl buffer, pH 7.4. Solid line, non-aged peptide; and dashed line, peptides aged for 24 h.

bond arrangements [29,30]. In FT-IR spectral analysis (Fig. 5A), β-sheets exhibit major amide I bands at 1620–1640 cm^{-1} as compared with α-helices with absorption at 1650–1658 cm^{-1}. The spectra obtained for non-aged glucagon showed only a small β-sheet intensity at 1620–1630 cm^{-1}, and aging treat-

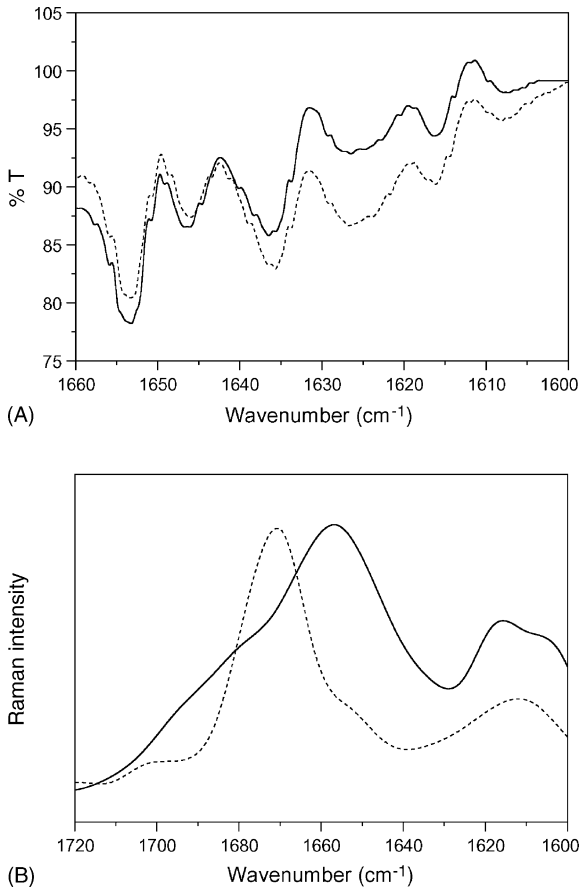

Fig. 5. Spectroscopic analyses of aged or non-aged glucagon. The amide I region of FT-IR (A) and Raman spectra (B) of age or non-aged glucagon. Glucagon was dissolved in 0.01 M HCl at the concentration of 5.0 mg/ml, and aged for 24 h at 37 °C. Aged glucagon solution was lyophilized and then applied for the spectroscopic analyses. Solid line, non-aged peptide; and dashed line, peptides aged for 24 h.

ment resulted in progressively greater amounts of β-sheet. On the basis of the deconvoluted and curve-fitted amide I band of the normal and aged glucagon, changes in the composition of each component were confirmed from 54% to 22% for α-helix/random coil structures and from 2% to 49% for β-sheet structure, respectively.

In addition to FT-IR spectrum, the Raman spectrum of peptides/proteins in the amide I region (1600–1700 cm^{-1}) tends to show high intensity and little interference from other group vibrations and is susceptive to the protein conformational changes [31]. Although there are other Raman bands including the amide II region (1400–1500 cm^{-1}) and amide III region (1200–1300 cm^{-1}), often used as marker bands for identifying the protein structure, these bands suffer interference from bands from the side groups of amino acids and make it difficult to analyze the conformation transition of the protein [32]. This is a part of reason why the amide I region has been used widely to estimate the secondary structure elements of proteins, and α-helical and β-sheet structure give rise to the amide I feature at 1645–1657 and 1665–1680, respectively [30]. When aged at 5.0 mg/ml for 24 h, the amide I band of the glucagon shift from 1657 to 1671 cm^{-1}, indicating that the β-sheet conformation increased in glucagon during aging treatment (Fig. 5B). This was consistent with the results from CD and FT-IR spectroscopic analyses.

It is well-established that the structural transition from α-helix to β-sheet is the main conformational characteristic in the aggregation process of amyloidogenic peptides/proteins including $A\beta_{1–42}$ [33], PrP [34], and human calcitonin [35]. In this study, it was shown that the aged glucagon possessed the same amyloidogenic conformational properties of β-sheet transition as amylin on the basis of the results from TEM, CD, FT-IR and Raman spectral analyses, while secretin, having 52% sequential homology with glucagon, did not. In addition to the primary structure, the solution structure of secretin and glucagon was also quite similar, showing the N-terminal short disordered structure and C-terminal long α-helical structure [18,26,27]. The amino acid sequences of the N-terminal disordered structure of these peptides, encompassing residues 1–8 or 9, are very similar, so it is assumed that differences in the aggregation properties of these peptides may be associated with their helical structures in the C-terminus, which display relatively lower sequential homology as compared to the N-terminus. Under highly concentrated conditions, the hydrophobic side groups of amyloidogenic peptides partially tend to huddle partially together to avoid the aqueous environment [36], and the hydrophobic interactions within their respective α-helical regions may initiate aggregation. According to X-ray analysis [36], the α-helical structure of glucagon, located in its amino acid sequence between positions 10 and 25, tends to interact each other through contacts between the sidechains of Trp at position 25, Phe at 22, and Tyr at 10 and 13. It should be noted that the corresponding amino acids in the sequence of secretin were all substituted by other residues, such as Gly at 25, Leu at 10, 13 and 22. It is suggested that the replacement of these amino acids brings about differences in the aggregation behavior between glucagon and secretin.

3.3. Capillary electrophoresis

CE has the potential to separate different conformations based on their radii of gyration or charge state [37], and the technique may allow the glucagon and its aggregates to be resolved. Initially, glucagon was dissolved in 50 mM phosphate buffer (pH 3.0) at the concentration of 1 mg/ml, and aged at 37 °C. The electropherograms of non-aged glucagon showed a single electrophoretic peak (Fig. 6A), and additional CE measurements were conducted after time intervals ranging from 0 to 28 h to test for the monitoring of glucagon aggregation. Glucagon aged for over 5 h displayed some unidentified peaks with slow electrophoretic mobility (arrowed in Fig. 6A), and a dramatical decrease in the glucagon peak was observed at 28 h. The electropherogram of glucagon aged at the concentration of 2.5 mg/ml for 3 h was also comprised of glucagon peak and delayed sharp (5.2 min) and small (7 min) peaks (Fig. 6B). These unidentified peaks, appeared in aged glucagon, were transient, and they as well as glucagon peak disappeared eventually. Considering the high aggregation potential of glucagon to form oligomeric species in the fibrilogenic process, it is feasible to assume that

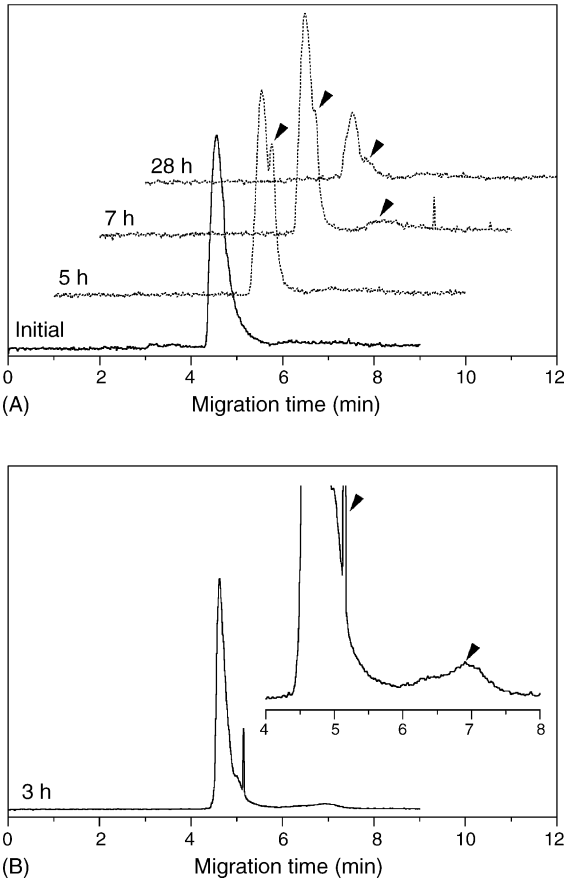

Fig. 6. Electrophoretic profiles of aged glucagon. (A) Aged glucagon. Glucagon, dissolved in pH 3.0 buffer was incubated at the concentration of 1.0 mg/ml for 0, 5, 7, and 28 h at 37 °C, and each sample aged at the indicated periods was applied on CE. (B) Glucagon aged at the concentration of 2.5 mg/ml for 3 h. The elution profiles were determined by UV detection at 214 nm. Arrows indicate aggregate peaks appearing in the running buffer.

these peaks could be representative of different oligomerization states of glucagon monomers. Thus, arrowed peaks in Fig. 6A and B have a slow electrophoretic mobility and it might be assigned as an oligomer of high molecular mass formed along the fibrillogenic pathway of the peptide. These findings were consistent with the results from CD spectral analysis, indicating that aged glucagon solution (pH 3.0) at 1.0 mg/ml for at least 5 h formed the aggregates with abundant β-sheet structure (data not shown).

Further CE experiments showed the kinetics of aggregation process (Figs. 7 and 8), which might depend on the dissolving conditions such as concentration of glucagon and pH. When aged at 1.0 mg/ml in pH 3.0 buffer, CE data showed ca. 20% decrease in a glucagon peak at 6 h, however aging treatment of glucagon at the concentration of 4.0 mg/ml resulted in a significant decrease in a glucagon peak within 5 h (Fig. 7). Hence, these CE analyses indicated that the aging at the higher concentrations accelerated the self-association of glucagon, producing amyloidogenic fibrils readily. With respect to the influence of pH on the aggregation behavior of glucagon, a time-dependent decrease in the amount of monomer with aging treatment of glucagon (1.0 mg/ml) was observed at pH 3.0 and 3.5, however, prior incubation of glucagon at 37 °C at pH 2.0 yielded only a slight change (Fig. 8). A linear relationship was obtained according to the following equation: $\ln A = \ln A_0 - kt$ (apparent first-order kinetics; $r = 0.991$), where A is the remaining peak area; k, the slope and t, the time (h). The aggregation rate was evaluated on the basis of kinetic constant k, with respect to the initial glucagon peak, and the following data were obtained: $k = 0.002$/h (95% confidence interval, −0.002 to 0.006/h) and 0.080/h (95% confidence interval, 0.069–0.091/h) for pH 2.0 and 3.5, respectively. Thus, aggregation rate of glucagon at pH 3.5 was found to be much higher than that at pH 2.0, suggesting that fibril formation of glucagon is strongly dependent on pH, with aggregation considerably faster as pH increased. This was further supported by the CD spectral experiments, showing that glucagon aged at pH 3.5 for 4 h had the β-sheet rich structure, but the aging of glucagon at pH 2.0 did not induce any conformational changes even after 24 h aging treatment (data not

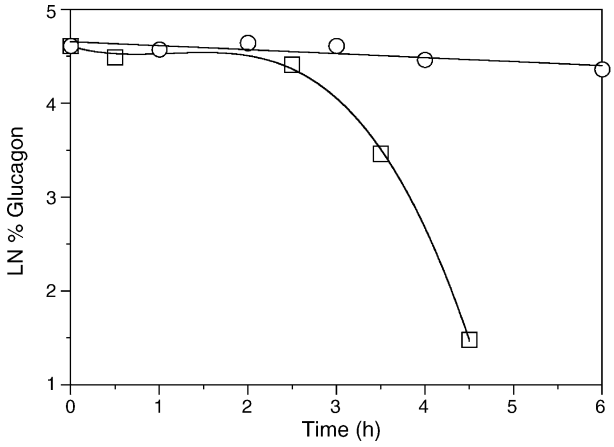

Fig. 7. The concentration dependent change in the relative normalized area of glucagon peaks during aging process. Glucagon, dissolved in pH 3.0 buffer, was incubated at the concentration of 1.0 mg/ml (◯) and 4.0 mg/ml (□) for indicated periods at 37 °C, and each sample aged at the indicated periods was applied on CE.

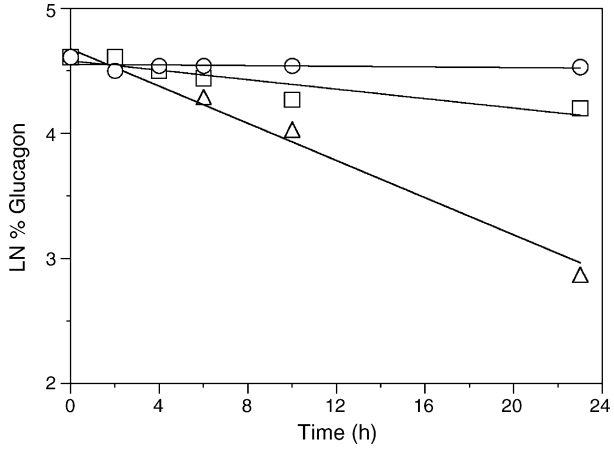

Fig. 8. The pH dependent change in the relative normalized area of glucagon peaks during aging process. Glucagon was dissolved in pH 2.0 (◯), pH 3.0 (□) and pH 3.5 (△) buffer, and each sample aged at the indicated periods was applied on CE.

shown). Generally, Asp residue has a pK_a around pH 3.0, and the presence of charge on the Asp and basic amino acid, including Lys and Arg, may form salt bridges in glucagon. Based on the results presented, Asp residues, as well as hydrophobic residues, in glucagon may play an important role in the self-association of glucagon, resulting in the formation of amyloid-like fibrils.

It is of interest to compare the result from CE experiments with the data on fibrillation of glucagon by other analytical technologies. We previously performed size exclusion chromatography (SEC) to check the size and molecular pattern of the glucagon aggregates [15]. The SEC analysis of the aged preparation showed two main peaks appeared at 3.5 and 2000 kDa for the glucagon monomer and glucagon aggregate, respectively. During the interval from the non-aging state to 6 h aging, the peak at 3.5 kDa of monomeric glucagon was shifted to generate a peak at 2000 kDa, suggesting that intermolecular association is likely to be involved in the generation of the glucagon aggregate. Although SEC analysis could detect the glucagon aggregates successfully, the monitoring of oligomeric intermediate during aging process has been failed. In contrast to SEC analysis, CE analysis of the aged glucagon could indicate the presence of some transient peaks, possibly corresponding to the oligomeric intermediates, that gradually decreased during aging treatment. In this context, CE could be a useful and reliable tool for the rapid monitoring of glucagon aggregation.

4. Conclusion

In this study, we demonstrated that the concentrated and aged glucagon possessed the same amyloidogenic conformational properties of β-sheet transition as amylin as confirmed by TEM, FT-IR, FT-Raman and CD spectral analyses, binding assays with Congo red, and CE analysis. As for porcine secretin, despite a high similarity in primary and secondary structural homology to glucagon, no transition of solution structure was observed after aging. These findings, taken together with the sequential difference and structural homology between secretin and glucagon, led to a hypothesis that some aromatic amino acid residues at the helical structure of glucagon may play a crucial role in the intermolecular hydrophobic interaction and initiation of aggregation.

On the basis of CE analysis, it was confirmed that the structural transition of glucagon was accelerated when glucagon solution was prepared at high concentration at pH 3.5, and CE analysis also successfully revealed the generation of aggregate intermediates during aging process. The approach using CE, as well as spectroscopic analyses, would be useful for characterizing the kinetics of peptides/proteins aggregation, which is of interest for the understanding of amyloidogenicity of glucagon and other peptides/proteins.

Acknowledgments

We wish to thank Yoshimi Itoh, Yoichi Saitoh, and Chizuko Fukuoka, Department of Analytical Chemistry, Faculty of Pharmaceutical Sciences, Toho University, for their excellent technical assistance throughout this work.

References

[1] G.G. Glenner, N. Engl. J. Med. 302 (1980) 1283.
[2] G.G. Glenner, N. Engl. J. Med. 302 (1980) 1333.
[3] G. Vines, Trends Biotechnol. 11 (1993) 49.
[4] G.J. Cooper, A.C. Willis, A. Clark, R.C. Turner, R.B. Sim, K.B. Reid, Proc. Natl. Acad. Sci. U.S.A. 84 (1987) 8628.
[5] S.B. Prusiner, Proc. Natl. Acad. Sci. U.S.A. 95 (1998) 13363.
[6] E. Scherzinger, R. Lurz, M. Turmaine, L. Mangiarini, B. Hollenbach, R. Hasenbank, G.P. Bates, S.W. Davies, H. Lehrach, E.E. Wanker, Cell 90 (1997) 549.
[7] J.D. Sipe, Annu. Rev. Biochem. 61 (1992) 947.
[8] S. Onoue, K. Ohshima, K. Endo, T. Yajima, K. Kashimoto, FEBS Lett. 522 (2002) 65.
[9] W.G. Turnell, J.T. Finch, J. Mol. Biol. 227 (1992) 1205.
[10] I.V. Kurochkin, FEBS Lett. 427 (1998) 153.
[11] M.J. Burke, M.A. Rougvie, Biochemistry 11 (1972) 2435.
[12] D.K. Clodfelter, A.H. Pekar, D.M. Rebhun, K.A. Destrampe, H.A. Havel, S.R. Myers, M.L. Brader, Pharm. Res. 15 (1998) 254.
[13] M. Cauchy, S. D'Aoust, B. Dawson, H. Rode, M. Hefford, Biologicals 30 (2002) 175.
[14] R.J. Ellis, T.J. Pinheiro, Nature 416 (2002) 483.
[15] S. Onoue, K. Ohshima, K. Debari, K. Koh, S. Shioda, S. Iwasa, K. Kashimoto, T. Yajima, Pharm. Res. 21 (2004) 1274.
[16] M. Rodbell, L. Birnbaumer, S.L. Pohl, F. Sundby, Proc. Natl. Acad. Sci. U.S.A. 68 (1971) 909.
[17] V. Mutt, J.E. Jorpes, S. Magnusson, Eur. J. Biochem. 15 (1970) 513.
[18] A.M. Gronenborn, G. Bovermann, G.M. Clore, FEBS Lett. 215 (1987) 88.
[19] D. Vaudry, B.J. Gonzalez, M. Basille, L. Yon, A. Fournier, H. Vaudry, Pharmacol. Rev. 52 (2000) 269.
[20] R.B. Merrifield, Adv. Enzymol. Relat. Areas Mol. Biol. 32 (1969) 221.
[21] R.W. Sarver Jr., W.C. Krueger, Anal. Biochem. 194 (1991) 89.
[22] W.E. Klunk, J.W. Pettegrew, D.J. Abraham, J. Histochem. Cytochem. 37 (1989) 1273.
[23] J. Cort, Z. Liu, G. Lee, S.M. Harris, K.S. Prickett, L.S. Gaeta, N.H. Andersen, Biochem. Biophys. Res. Commun. 204 (1994) 1088.
[24] G. Forloni, N. Angeretti, R. Chiesa, E. Monzani, M. Salmona, O. Bugiani, F. Tagliavini, Nature 362 (1993) 543.
[25] B. Solomon, R. Koppel, E. Hanan, T. Katzav, Proc. Natl. Acad. Sci. U.S.A. 93 (1996) 452.
[26] R.M. Robinson, E.W. Blakeney Jr., W.L. Mattice, Biopolymers 21 (1982) 1271.
[27] W. Braun, G. Wider, K.H. Lee, K. Wuthrich, J. Mol. Biol. 169 (1983) 921.
[28] N. Greenfield, G.D. Fasman, Biochemistry 8 (1969) 4108.
[29] W.K. Surewicz, H.H. Mantsch, Biochim. Biophys. Acta 952 (1988) 115.
[30] H. Fabian, P. Anzenbacher, Vib. Spectrosc. 4 (1993) 125.
[31] J. Kubelka, P. Pancoska, T. Keiderling, Appl. Spectrosc. 53 (1999) 666.
[32] X.H. Zong, P. Zhou, Z.Z. Shao, S.M. Chen, X. Chen, B.W. Hu, F. Deng, W.H. Yao, Biochemistry 43 (2004) 11932.
[33] N. Demeester, C. Mertens, H. Caster, M. Goethals, J. Vandekerckhove, M. Rosseneu, C. Labeur, Eur. J. Neurosci. 13 (2001) 2015.
[34] K.M. Pan, M. Baldwin, J. Nguyen, M. Gasset, A. Serban, D. Groth, I. Mehlhorn, Z. Huang, R.J. Fletterick, F.E. Cohen, et al., Proc. Natl. Acad. Sci. U.S.A. 90 (1993) 10962.
[35] M. Kamihira, A. Naito, S. Tuzi, A.Y. Nosaka, H. Saito, Protein Sci. 9 (2000) 867.
[36] K. Sasaki, S. Dockerill, D.A. Adamiak, I.J. Tickle, T. Blundell, Nature 257 (1975) 751.
[37] B. Verzola, F. Chiti, G. Manao, P.G. Righetti, Anal. Biochem. 282 (2000) 239.